

AN INVESTIGATION OF HIGHER-ORDER CLOSURE MODELS FOR A FORESTED CANOPY

GABRIEL G. KATUL¹ and JOHN D. ALBERTSON²

¹*School of the Environment, Duke University, Durham, NC 27708-0328;* ²*Department of Environmental Sciences, University of Virginia, Charlottesville, VA 22903*

(Received in final form 31 March 1998)

Abstract. Simultaneous triaxial sonic anemometer velocity measurements vertically arrayed at six levels within and above a uniform pine forest were used to examine two parameterization schemes for the triple-velocity correlation tensor employed in higher-order closure models. These parameterizations are the gradient-diffusion approximation typically used in second-order closure models, and the full budget for the triple-velocity correlation tensor typically employed in third-order closure models. Both second- and third-order closure models failed to reproduce the measured profiles of the triple-velocity correlation within and above the canopy. However, the Reynolds stress tensor profiles (including velocity variances) deviated greatly from the measurements only within the lower levels of the canopy. It is shown that the Reynolds stresses are most sensitive to the parameterization of the triple-velocity correlation in these lower canopy regions where local turbulent production is negligible and turbulence is mainly sustained by the flux transport term. The failure of the third-order closure model to reproduce the measured third moments in the upper layers of the canopy-top contradicts conclusions from a previous study over shorter vegetation but agrees with another study for a deciduous forest. Whether the third-order closure model failure is due to the zero-fourth-cumulant closure approximation is therefore considered. Comparisons between measured and predicted quadruple velocity correlations suggest that the zero-fourth-cumulant approximation is valid close to the canopy-atmosphere in agreement with recent experiments.

Keywords: Canopy closure model, Pine forest, Turbulence.

1. Introduction

It has been demonstrated that scalar sources, sinks, and fluxes can be successfully related to mean scalar concentration profiles within the canopy sub layer (CSL) via particle trajectory and Lagrangian dispersion models if vertical profiles of the velocity statistics are known (e.g., Leclerc et al., 1988; Raupach et al., 1992; Baldocchi, 1992; Katul et al., 1997a). One-dimensional canopy flow models, capable of reproducing many features of the velocity statistics profiles needed in Lagrangian models, have been developed over the past three decades with varying complexity, limitations, and successes. These models range from conventional mixing length models of eddy viscosity (Cionco, 1965, 1972; Cowan, 1968; Thom, 1971; Halldin and Lindroth, 1986) to higher-order closure models.

Limitations of first-order closure are well recognized (Shaw, 1977; Raupach, 1988; Wilson, 1989) though they are still widely employed in many research ar-



eas such as: satellite-based observations of land-surface processes (Taconet et al., 1986); circulation and mesoscale models (Sellers et al., 1986); the determination of canopy aerodynamic properties such as zero-plane displacement, momentum roughness heights, and drag coefficients (e.g., Kondo and Akashi, 1976; Albini, 1981; Massman, 1987, 1997; Raupach, 1994). First-order closure models that introduce non-local contributions to the eddy viscosity have been proposed (e.g., Li et al., 1985), but such models typically require six empirical constants and heuristic parameterizations of the non-local contributions. Furthermore, such models are based on the mean longitudinal momentum equation and cannot predict the variances required by Lagrangian dispersion models. Closure at higher order is necessary for modelling velocity variance profiles as needed in Lagrangian stochastic models. Second-order closure models have been proposed and successfully tested for short vegetation and, to a much lesser extent, forest stands (Wilson and Shaw, 1977; Lewellen et al., 1980; Wilson, 1988).

A deficiency of second-order closure models is the flux-gradient approximation of the triple-velocity correlation (Deardorff, 1978), which for canopy flows produces unrealistic momentum flux transport profiles near the canopy top. Meyers and Paw U (1986) proposed a third-order closure budget for the triple-velocity correlation, which related the fourth moment to second moments using a zero-fourth cumulant expansion. For a maize canopy, Meyers and Paw U (1986) reported good agreement between triple-velocity correlation predictions and measurements. However, it appears that the second-order closure model of Wilson and Shaw (1977) produced velocity variance estimates that are in closer agreement to measurements for a similar maize canopy than the closure model predictions of Meyers and Paw U (1986). Whether the inclusion of a budget for the triple-velocity correlation tensor is a significant improvement over the flux-gradient approximation remains questionable, especially if the closure model objectives are to predict velocity variance profiles. Such comparisons are clouded by the additional difference in the models of Meyers and Paw U (1986) and Wilson and Shaw (1977) with respect to the pressure-velocity covariance parameterization, the latter using the form proposed by Mellor (1973) and the former using parameterizations from Zeman and Lumley (1976) and Zeman and Tennekes (1975). Hence, from the published results alone, it is difficult to discern model improvements due solely to increasing closure order for the triple-velocity correlation tensor. In fact, the decision as to what order to close the equations for modelling second moments is inherent in all closure modeling of high Reynolds number flows. The addition of budgets for third- and higher-order moments does not always translate to improved predictions of first and second moments given the difficulties in constructing “realizable” closure models for these higher moments (Launder, 1996; Lumley, 1978; Schumann, 1977).

The primary objective of this study is to investigate whether third-order closure produces second-order velocity statistics profiles that are in closer agreement with measurements when compared to those computed via a flux-gradient approxima-

tion (second-order closure) in a forest stand. For this purpose, an experiment was carried out in a 14 year old even-aged pine forest with a significant understory component. Six sonic anemometers simultaneously measured all the velocity components within and above the canopy for a wide range of wind and shear stress conditions at the canopy top. A third-order closure model, with a triple-velocity correlation budget identical to the budget of Meyers and Paw U (1986), but with all other components of the Reynolds stress budget retained from the Wilson and Shaw (1977) model, was used. The profiles of mean velocity, momentum flux, velocity variances, components of the turbulent kinetic energy budget, and triple-velocity correlations modelled from second- and third-order closure approximations were compared with measurements from the pine forest. The outcome from this comparison will guide modeling the velocity statistics within the canopy for use in Lagrangian dispersion models that estimate sources, sinks, and turbulent scalar fluxes from mean scalar concentration profiles as in Raupach (1989) and Katul et al. (1997a). Furthermore, the ability of such closure models to predict third-order moments potentially used as inputs in random flight particle trajectory models is also considered.

2. Theory

For a steady state, adiabatic flow, the time and horizontally averaged equations for momentum and Reynolds stresses are:

$$\begin{aligned}
\frac{\partial \langle \bar{u}_i \rangle}{\partial t} &= 0 = -\frac{\partial \langle \bar{u}'_i \bar{u}'_j \rangle}{\partial x_j} - \left(\left\langle \frac{\partial \bar{p}}{\partial x_i} \right\rangle + \left\langle \frac{\partial \bar{p}''}{\partial x_i} \right\rangle \right) \\
&\quad + \nu \left(\frac{\partial^2 \langle \bar{u}_i \rangle}{\partial x_j \partial x_j} + \left\langle \frac{\partial^2 \bar{u}_i''}{\partial x_j \partial x_j} \right\rangle \right) - \left\langle \bar{u}_j \frac{\partial \bar{u}_i}{\partial x_j} \right\rangle \\
\frac{\partial \langle \bar{u}'_i \bar{u}'_k \rangle}{\partial t} &= 0 = - \left(\overline{\langle u'_j u'_k \rangle} \frac{\partial \langle \bar{u}_i \rangle}{\partial x_j} + \overline{\langle u'_i u'_j \rangle} \frac{\partial \langle \bar{u}_k \rangle}{\partial x_j} \right) \\
&\quad - \left(\frac{\partial \langle \bar{u}'_i \bar{u}'_j \bar{u}'_k \rangle}{\partial x_j} \right) - \left(\left\langle \overline{u'_k \frac{\partial p'}{\partial x_i}} \right\rangle + \left\langle \overline{u'_i \frac{\partial p'}{\partial x_k}} \right\rangle \right) \\
&\quad + \left(\langle \bar{u}_k \rangle \left\langle \frac{\partial \bar{p}''}{\partial x_i} \right\rangle + \langle \bar{u}_i \rangle \left\langle \frac{\partial \bar{p}''}{\partial x_k} \right\rangle \right) \\
&\quad + \nu \left(-2 \left\langle \frac{\partial \bar{u}'_i \bar{u}'_j \bar{u}'_k}{\partial x_j \partial x_j} \right\rangle + \frac{\partial^2 \langle \bar{u}_i'' \bar{u}_k'' \rangle}{\partial x_j \partial x_j} \right), \tag{1}
\end{aligned}$$

where x_i ($x_1 = x$, $x_2 = y$, $x_3 = z$) are the longitudinal, lateral, and vertical directions, respectively, u_i ($u_1 = u$, $u_2 = v$, $u_3 = w$) are the instantaneous velocity components along x_i , p is the static pressure normalized by the air density, ν is the

kinematic viscosity, $(\bar{\cdot})$ and $\langle \cdot \rangle$ denote time and horizontal averaging, respectively, primes and double primes denote departures from the temporal and horizontal averaging operators, respectively, as discussed in Raupach and Shaw (1982). All double primed terms in (1) arise because of horizontal averaging the multiply-connected air spaces within the vegetation volume; hence, they are directly related to vegetation effects on the flow statistics.

2.1. SECOND-ORDER CLOSURE APPROXIMATIONS OF WILSON AND SHAW (1977)

In Wilson and Shaw (1977), the closure approximations for the mean momentum equations are:

$$\begin{aligned} \left\langle \frac{\partial \bar{p}'}{\partial x_i} \right\rangle &= C_d A \langle \bar{u}_i \rangle^2 \\ \nu \left\langle \frac{\partial^2 \bar{u}_i''}{\partial x_j \partial x_j} \right\rangle &= 0. \end{aligned} \quad (2)$$

Such an approximation assumes that the form-drag by the canopy can be modeled as a general drag force and that the viscous drag can be neglected (relative to the form drag), and it employs C_d as a drag coefficient, and A as the plant area density at height x_3 . The closure for the Reynolds stress equations are similar to those proposed by Mellor (1973):

$$\begin{aligned} \langle \bar{u}_i' \bar{u}_j' \bar{u}_k' \rangle &= -q \lambda_1 \left(\frac{\partial \langle \bar{u}_i' \bar{u}_j' \rangle}{\partial x_k} + \frac{\partial \langle \bar{u}_j' \bar{u}_i' \rangle}{\partial x_i} + \frac{\partial \langle \bar{u}_k' \bar{u}_i' \rangle}{\partial x_j} \right) \\ \left\langle \bar{u}_i' \frac{\partial p'}{\partial x_k} \right\rangle + \left\langle \bar{u}_k' \frac{\partial p'}{\partial x_i} \right\rangle &= - \left\langle p' \frac{\partial \bar{u}_i'}{\partial x_k} \right\rangle - \left\langle p' \frac{\partial \bar{u}_k'}{\partial x_i} \right\rangle + \left\langle \frac{\partial p' \bar{u}_i'}{\partial x_k} \right\rangle + \left\langle \frac{\partial p' \bar{u}_k'}{\partial x_i} \right\rangle \\ \left\langle p' \frac{\partial \bar{u}_i'}{\partial x_k} \right\rangle + \left\langle p' \frac{\partial \bar{u}_k'}{\partial x_i} \right\rangle &= - \frac{q}{3 \lambda_2} \left[\langle \bar{u}_i' \bar{u}_k' \rangle - \delta_{ik} \frac{q^2}{3} \right] + C q^2 \left[\frac{\partial \langle \bar{u}_i \rangle}{\partial x_k} + \frac{\partial \langle \bar{u}_k \rangle}{\partial x_i} \right] \\ \left\langle \frac{\partial p' \bar{u}_i'}{\partial x_k} \right\rangle + \left\langle \frac{\partial p' \bar{u}_k'}{\partial x_i} \right\rangle &= 0 \\ 2\nu \left(\left\langle \frac{\partial \bar{u}_i'}{\partial x_j} \frac{\partial \bar{u}_k'}{\partial x_j} \right\rangle \right) &= \frac{2 q^3}{3 \lambda_3} \delta_{ik} = \frac{2}{3} \langle \varepsilon \rangle \delta_{ik}, \end{aligned} \quad (3)$$

where $q = \sqrt{\langle \bar{u}_i' \bar{u}_i' \rangle}$ is a characteristic turbulent velocity, $\langle \varepsilon \rangle$ is the mean rate of viscous dissipation, λ_1 , λ_2 , and λ_3 are characteristic length scales for the triple-velocity correlation, the pressure-velocity gradient correlations, and the viscous

dissipation, respectively, and C is a constant to be determined. As with typical second-order closure models, the triple-velocity products are closed using a gradient diffusion approximation, the pressure-velocity gradients are modeled on return-to-isotropy principles following Mellor (1973) and Donaldson (1973), and the viscous dissipation is assumed isotropic and dependent on the local turbulence intensity (Mellor, 1973). Upon replacing these approximations in Equation (1), and assuming horizontal homogeneity and steady state, the Wilson and Shaw (1977) model simplifies to:

$$\begin{aligned}
0 &= \frac{d\langle \overline{u'w'} \rangle}{dz} - C_d A \langle \bar{u} \rangle^2 \\
0 &= -\langle \overline{w'^2} \rangle \frac{d\langle \bar{u} \rangle}{dz} + 2 \frac{d}{dz} \left(q \lambda_1 \frac{d\langle \overline{u'w'} \rangle}{dz} \right) - \frac{q \langle \overline{u'w'} \rangle}{3 \lambda_2} + C q^2 \frac{d\langle \bar{u} \rangle}{dz} \\
0 &= -2 \langle \overline{u'w'} \rangle \frac{d\langle \bar{u} \rangle}{dz} + \frac{d}{dz} \left(q \lambda_1 \frac{d\langle \overline{u'^2} \rangle}{dz} \right) \\
&\quad + 2 C_d A \langle \bar{u} \rangle^3 - \frac{q}{3 \lambda_2} \left(\langle \overline{u'^2} \rangle - \frac{q^2}{3} \right) - \frac{2 q^3}{3 \lambda_3} \\
0 &= \frac{d}{dz} \left(q \lambda_1 \frac{d\langle \overline{v'^2} \rangle}{dz} \right) - \frac{q}{3 \lambda_2} \left(\langle \overline{v'^2} \rangle - \frac{q^2}{3} \right) - \frac{2 q^3}{3 \lambda_3} \\
0 &= \frac{d}{dz} \left(3 q \lambda_1 \frac{d\langle \overline{w'^2} \rangle}{dz} \right) - \frac{q}{3 \lambda_2} \left(\langle \overline{w'^2} \rangle - \frac{q^2}{3} \right) - \frac{2 q^3}{3 \lambda_3},
\end{aligned} \tag{4}$$

with

$$\lambda_j = a_j L(z); \quad j = 1, 2, 3$$

$$L(z) = \max \begin{cases} L(z - dz) + k dz \\ \frac{\alpha}{C_d A} \end{cases}$$

$$L(0) = 0,$$

where $k (= 0.4)$ is von Karman's constant, α is a constant to be determined experimentally, a_1, a_2, a_3 and C can be determined such that the flow conditions well above the canopy reproduce established surface-layer similarity relations (Monin and Yaglom, 1971), and dz is the depth increment. With estimates of the five constants (a_1, a_2, a_3, C , and α), the five ordinary differential equations in Equation (4) can be solved iteratively for the five flow variables $\langle \bar{u} \rangle, \langle \overline{u'w'} \rangle, \langle \overline{u'^2} \rangle, \langle \overline{v'^2} \rangle,$

$\overline{\langle w'^2 \rangle}$. Details of the computational technique and determination of the constants are presented in Appendix A.

2.2. THIRD-ORDER CLOSURE APPROXIMATIONS

A primary weakness in higher-order closure models is the gradient diffusion approximation for the triple-velocity correlation (see e.g., Deardorff, 1978; Sreenivasan et al., 1982; Raupach, 1988). In particular, the closure scheme proposed by Mellor (1973) and used by Wilson and Shaw (1977) results in zero flux transport just above the canopy, which contrasts with laboratory and field measurements collected over a wide range of roughness and morphologically different canopy stands (Nakagawa and Nezu, 1977; Mulhearn and Finnigan, 1978; Maitani, 1978; Raupach, 1981; Shaw et al., 1983; Meyers and Paw U, 1986; Nagano and Tagawa, 1990, 1996; Raupach et al., 1991; Katul et al., 1997b). Meyers and Paw U (1986) proposed a simplified budget for one plane out of the third-order tensor (referred to here as triple-velocity correlation) and used a zero-fourth cumulant approximation to relate fourth and second moments (see Appendix B). For a horizontally homogeneous flow, this budget reduces to:

$$\begin{aligned}
0 = & -\overline{\langle u'_i w' w' \rangle} \frac{\partial \langle \overline{u_j} \rangle}{\partial z} - \overline{\langle u'_j w' w' \rangle} \frac{\partial \langle \overline{u_i} \rangle}{\partial z} \\
& - \overline{\langle w'^2 \rangle} \frac{\partial \langle \overline{u'_i u'_j} \rangle}{\partial z} - \overline{\langle u'_i w' \rangle} \frac{\partial \langle \overline{w' u'_j} \rangle}{\partial z} - \overline{\langle u'_j w' \rangle} \frac{\partial \langle \overline{w' u'_i} \rangle}{\partial z} \\
& - \left\langle \overline{u'_i u'_j} \frac{\partial p'}{\partial z} \right\rangle - \left\langle \overline{u'_i w'} \frac{\partial p'}{\partial x_j} \right\rangle - \left\langle \overline{u'_j w'} \frac{\partial p'}{\partial x_i} \right\rangle \\
& + \overline{\langle u'_i w' \rangle} \left\langle \frac{\partial \overline{p''}}{\partial x_j} \right\rangle + \overline{\langle u'_j w' \rangle} \left\langle \frac{\partial \overline{p''}}{\partial x_i} \right\rangle - M_{ij3}; \\
M_{ij3} = & 2\nu \left\langle \overline{w' \frac{\partial u'_i}{\partial x_k} \frac{\partial u'_j}{\partial x_k}} + \overline{u'_j \frac{\partial u'_i}{\partial x_k} \frac{\partial w'}{\partial x_k}} + \overline{u'_i \frac{\partial u'_j}{\partial x_k} \frac{\partial w'}{\partial x_k}} \right\rangle.
\end{aligned} \tag{5}$$

In the triple-velocity correlation budget, closure is achieved by parameterizing the pressure and molecular terms using a simplified return-to-isotropy scheme proposed by André et al. (1981):

$$\left\langle \overline{u'_i u'_j} \frac{\partial p'}{\partial z} \right\rangle + \left\langle \overline{u'_i w'} \frac{\partial p'}{\partial x_j} \right\rangle + \left\langle \overline{u'_j w'} \frac{\partial p'}{\partial x_i} \right\rangle + M_{ij3} = \frac{C_8 \overline{\langle w' u'_i u'_j \rangle}}{\tau}$$

where C_8 is a constant ($C_8 = 9$ in Meyers and Paw U, 1986, and $C_8 = 8$ in André et al., 1981; the subscript 8 is used for notational consistency with other studies),

and $\tau = q^2/\langle \varepsilon \rangle$ is a relaxation time scale. We note that the original formulation of André et al. (1981) did not include the dissipative part ($= M_{ij3}$). Terms involving $\langle \partial \overline{p''}/\partial x_i \rangle$ are parameterized as in Wilson and Shaw (1977) using the drag force analogy.

For consistency in closure model comparisons, we revised the Meyers and Paw U (1986) Reynolds stress equations so that the pressure-velocity correlation is modeled after Wilson and Shaw (1977) rather than Zeman and Lumley (1976) and Zeman and Tennekes (1975). The dissipation term in both Wilson and Shaw (1977) and Meyers and Paw U (1986) are identical. Hence, the primary difference between the two closure models studied here is the addition of a budget for the triple-velocity correlation. With such closure approximations, the modified third-order closure model of Meyers and Paw U (1986) can be written as:

$$\begin{aligned}
0 &= -\frac{d\langle \overline{u'w'} \rangle}{dz} - C_d A \langle \overline{u} \rangle^2 \\
0 &= -\langle \overline{w'^2} \rangle \frac{d\langle \overline{u} \rangle}{dz} - \frac{d}{dz} (\langle \overline{w'u'w'} \rangle) - \frac{q\langle \overline{u'w'} \rangle}{3\lambda_2} + Cq^2 \frac{d\langle \overline{u} \rangle}{dz} \\
0 &= -2\langle \overline{u'w'} \rangle \frac{d\langle \overline{u} \rangle}{dz} - \frac{d}{dz} (\langle \overline{w'u'w'} \rangle) + 2C_d A \langle \overline{u} \rangle^3 \\
&\quad - \frac{q}{3\lambda_2} \left(\langle \overline{u'^2} \rangle - \frac{q^2}{3} \right) - \frac{2q^3}{3\lambda_3} \\
0 &= -\frac{d}{dz} (\langle \overline{w'v'v'} \rangle) - \frac{q}{3\lambda_2} \left(\langle \overline{v'^2} \rangle - \frac{q^2}{3} \right) - \frac{2q^3}{3\lambda_3} \\
0 &= -\frac{d}{dz} (\langle \overline{w'w'w'} \rangle) - \frac{q}{3\lambda_2} \left(\langle \overline{w'^2} \rangle - \frac{q^2}{3} \right) - \frac{2q^3}{3\lambda_3} \\
\langle \overline{w'u'u'} \rangle &= -\frac{\tau}{C_8} \left(2\langle \overline{w'u'w'} \rangle \frac{d\langle \overline{u} \rangle}{dz} + \langle \overline{w'^2} \rangle \frac{d\langle \overline{u'^2} \rangle}{dz} - 4\langle \overline{u'w'} \rangle C_d A \langle \overline{u} \rangle^2 \right) \\
\langle \overline{w'u'w'} \rangle &= -\frac{\tau}{C_8} \left(2\langle \overline{w'w'w'} \rangle \frac{d\langle \overline{u} \rangle}{dz} + \langle \overline{w'u'} \rangle \frac{d\langle \overline{w'^2} \rangle}{dz} - 3\langle \overline{w'^2} \rangle C_d A \langle \overline{u} \rangle^2 \right) \\
\langle \overline{w'w'w'} \rangle &= -\frac{\tau}{C_8} \left(3\langle \overline{w'^2} \rangle \frac{d\langle \overline{w'^2} \rangle}{dz} \right) \\
\langle \overline{w'v'v'} \rangle &= -\frac{\tau}{C_8} \left(\langle \overline{w'^2} \rangle \frac{d\langle \overline{v'^2} \rangle}{dz} \right). \tag{6}
\end{aligned}$$

This system of equations can be solved numerically for the nine unknowns $\langle \bar{u} \rangle$, $\langle \overline{u'w'} \rangle$, $\langle \overline{u'^2} \rangle$, $\langle \overline{v'^2} \rangle$, $\langle \overline{w'^2} \rangle$, $\langle \overline{w'u'w'} \rangle$, $\langle \overline{w'u'u'} \rangle$, $\langle \overline{w'v'v'} \rangle$, $\langle \overline{w'w'w'} \rangle$. Note that the zero-fourth cumulant approximation as applied to the triple-velocity correlation budget yielded a flux-gradient parameterization for $\langle \overline{w'v'v'} \rangle$ and $\langle \overline{w'w'w'} \rangle$. Nonetheless, the terms $\langle \overline{w'u'u'} \rangle$ and $\langle \overline{w'u'w'} \rangle$, include both ‘local’ gradients (e.g., $d\langle \overline{u'^2} \rangle/dz$ and $d\langle \overline{w'^2} \rangle/dz$) and ‘non-local’ contributions modelled in terms of $\langle \bar{u} \rangle^2$. The closure models in Equations (4) and (6) were applied to the pine forest stand and compared to the velocity measurements described next.

3. Experiment Setup

3.1. THE SITE

An experiment was carried out from May 25, 1997 until June 11, 1997 at the Blackwood division of the Duke Forest near Durham, North Carolina (35°98' N, 79°8' W, elevation = 163 m). The site is an even-aged loblolly pine stand, established from seedlings planted at 2.4 by 2.4 m spacing in 1983 following clear-cutting and burning. Details about the site, understory species composition, and general climatic conditions can be found in Ellsworth et al. (1995) and Katul et al. (1997a). The site is equipped with a 20 m tall aluminum walkup tower. The average canopy height (h) neighboring the tower is 14 m (± 0.5 m).

3.2. INSTRUMENT SETUP

The three velocity components (u_i) and virtual potential temperature (T_a) were measured at six heights using five Campbell Scientific *CSAT3* triaxial sonic anemometers (sonic path length = 10 cm) and a *Solent Gill* sonic anemometer (sonic path length = 14.9 cm). The *CSAT3* sonic anemometers were positioned at $z = 4.15, 5.95, 9.65, 13.16,$ and 15.91 m above the soil surface. The *CSAT3* anemometer transducer heads were positioned at least 60 cm from the nearest foliage to avoid sonic wave interference from leaves. One *Solent Gill* anemometer was mounted on a short boom attached to the tower, at 20.70 m above the ground surface. A comparison between the *CSAT3* and the *Solent Gill* sonic anemometers was performed on October 11–13, 1997, to assess any systematic biases between the two sonic designs. The two anemometers were positioned at $z/h = 1.14$ separated by 0.9 m horizontally. The comparison, shown in Table I, demonstrates that no systematic biases in the turbulent velocity statistics arise from using these sonic anemometer types.

TABLE I

Comparison between the *CSAT3* and the *Solent Gill* anemometer (SG) velocity statistics at $z/h = 1.14$ for 88 half-hour runs. The regression model $y = Ax + B$ is used to assess systematic biases in measured flow statistics, where y are the *CSAT3* and x are the SG measured flow statistics. For completeness, the mean air temperature ($\langle T \rangle$), the temperature standard deviation (σ_T), and the sensible heat flux (H) are shown. The coefficient of determination (R^2) and the standard error of estimate (SEE) are also shown.

Variable	Slope (A)	Intercept (B)	R^2	SEE
$\langle \bar{u} \rangle$ (m s^{-1})	0.94	0.17	0.963	0.08
$\langle T \rangle$ ($^{\circ}\text{C}$)	1.26	-4.0	0.996	0.27
σ_u (m s^{-1})	0.99	0.03	0.993	0.02
σ_v (m s^{-1})	0.99	0.023	0.991	0.03
σ_w (m s^{-1})	0.99	-0.003	0.998	0.007
σ_T ($^{\circ}\text{C}$)	1.00	0.051	0.941	0.05
u_* (m s^{-1})	1.01	-0.007	0.980	0.02
H (W m^{-2})	1.04	0.53	0.992	7.05

3.3. DATA COLLECTION

All 24 analog signals were sampled at 10 Hz using a *CR9000* Campbell Scientific data logger positioned at the base of the tower, and saved by a portable computer. The experiment produced 171 runs, each representing a 30-minute sampling duration (18,000 measurements per flow variable, per run). Of the 171 runs, 64 runs were collected during night-time conditions and were excluded from the present analysis. The experiment resulted in 69 runs satisfying three criteria: (1) the mean wind direction was between 110° and 250° (minimizing tower interference for the *CSAT3* anemometers above the canopy), (2) the standard deviation of the wind direction did not exceed 50° , and (3) the u_* measured by the *Solent Gill* anemometer exceeded 0.15 m s^{-1} . The selected 69 runs form an ensemble at each height to which closure model predictions will be compared.

3.4. THE LEAF AREA INDEX (LAI) PROFILE MEASUREMENT

The shoot silhouette area index, a value analogous to the leaf area index (LAI), was measured in the vertical at 1 m intervals by a pair of *LICOR LAI 2000* plant canopy analyzers on June 4, 1997. The methods for converting shoot silhouette index to LAI for this stand is described in Ellsworth et al. (1995). The overall LAI for this stand is $3.82 \text{ m}^2 \text{ m}^{-2}$, with much of the foliage concentrated at $z = 8.5 \text{ m}$ (see Figure 1).

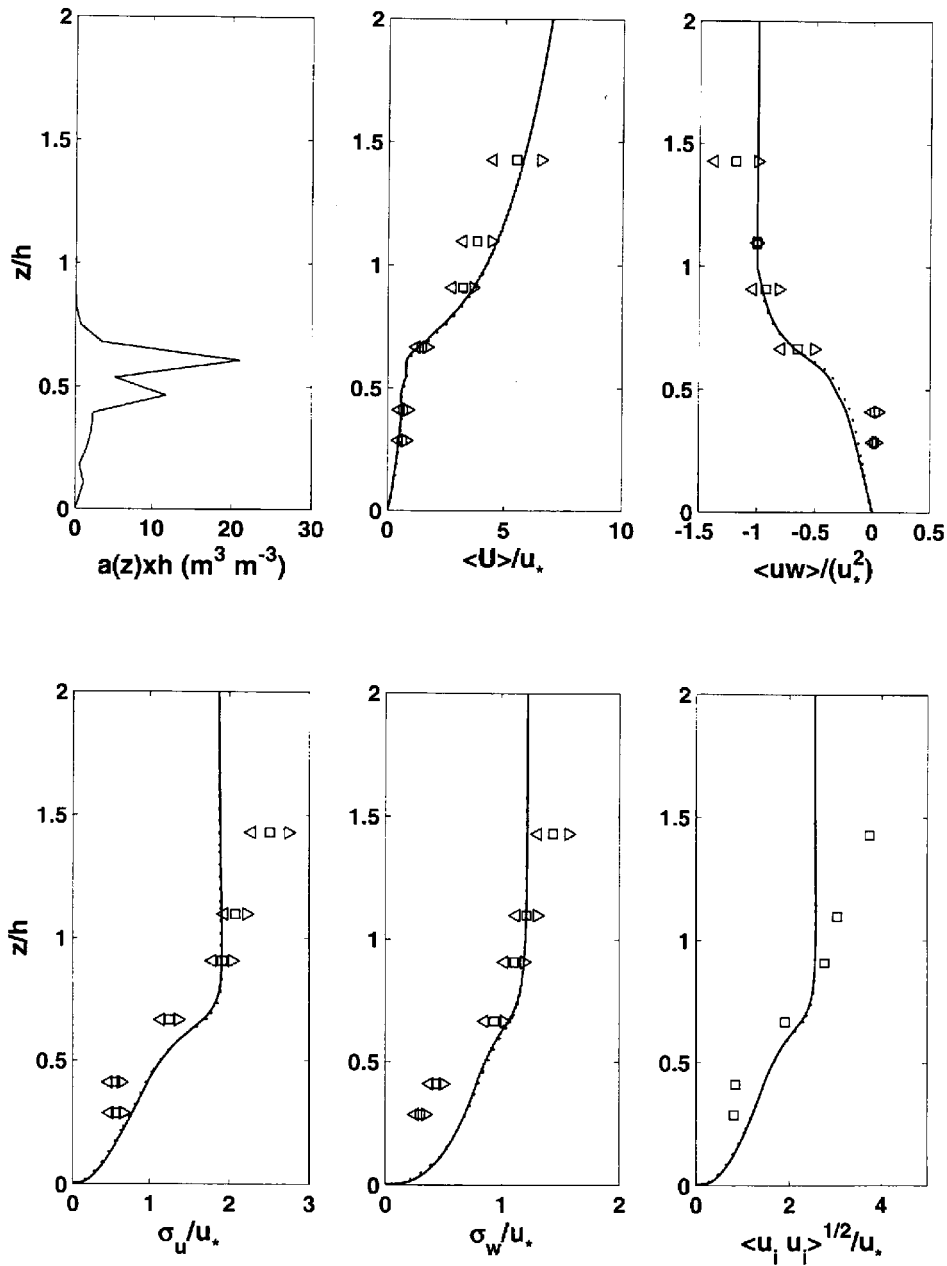


Figure 1. Comparison between modeled and measured profiles of $\langle \bar{u} \rangle$, $\overline{u'w'}$, $\overline{u'^2}^{1/2}$, $\overline{w'^2}^{1/2}$, and q . The solid line is for third-order closure, the dotted line is for second-order closure, u_* is defined at the canopy top ($z/h = 1$), and the squares are ensemble measurements from the 69 runs. The triangles are ± 1 standard deviation of normalized flow variables. The leaf area index profile (LAI) normalized by canopy height (h) is also shown (top left panel).

4. Results and Discussion

In this section, comparisons between third- and second-order closure model predictions and measurements are presented in order to assess whether closure beyond order two significantly improves the modeled profiles of $\langle \overline{u'_i u'_j} \rangle$. Furthermore, the zero-fourth cumulant approximations for the quadruple-velocity correlation tensor (see Appendix B) is examined with measurements to further assess whether such closure approximation is reasonable for CSL flows.

4.1. COMPARISONS WITH MEASUREMENTS

4.1.1. First and Second Moments

In Figure 1, the ensemble averages of the measured profiles of normalized LAI, $\langle \bar{u} \rangle$, $\langle \overline{u'w'} \rangle$, $\langle \overline{u'^2} \rangle^{1/2}$, $\langle \overline{w'^2} \rangle^{1/2}$, and q are shown with bounds of one standard deviation. As in all canopy sublayer field experiments, it is assumed here that the collection of time averages, when properly normalized, forms an ensemble of realizations. The modeled profiles from the second- and third-order closure models are also shown and compared to the measurements in Table II. Both models reproduce well the $\langle \bar{u} \rangle$, $\langle \overline{u'w'} \rangle$, $\langle \overline{u'^2} \rangle$, $\langle \overline{u'^2} \rangle^{1/2}$ profiles within the canopy ($z/h < 1$), but overestimate the $\langle \overline{w'^2} \rangle^{1/2}$ profile, especially for $z/h < 0.4$. Interestingly, this overestimation is also apparent in the model results of Meyers and Baldocchi (1991), Meyers and Paw U (1986), and Wilson and Shaw (1977). Furthermore, the mean momentum equations in Equations (4) and (6) produce a constant stress with height for $z/h > 1$, thus failing to reproduce the observed momentum flux increase above the canopy. What is important to note is that the difference between second- and third-order closure model predictions is not large with respect to the scatter in the measurements. Hence, from Table II, no apparent advantage to using the more complex parameterization of Meyers and Paw U (1986) over the simpler parameterization of Wilson and Shaw (1977) is evident.

4.1.2. Third-Order Moments

The success of random-flight models (RFM) to predict scalar transport in non-Gaussian turbulent flow fields is motivating the development of closure models for third-order moments (Raupach, 1988) that can be used in conjunction with RFM. Random-flight models use a generalized Langevin equation with non-Gaussian random forcing increments to model the particle trajectory (Sawford, 1986; Sawford and Guest, 1987). This is in contrast to the Gaussian random increments used in random-walk models. Hence, investigating how well higher-order closure models reproduce third moments is necessary prior to using them in RFM. In addition, the overestimation of $\langle \overline{w'^2} \rangle^{1/2}$ for $z/h < 0.4$ (discussed in Section 4.1.1) may well be related to the inability of these higher-order closure models to predict third

TABLE II

Comparison between eddy-covariance measured (EC) and closure model computed flow statistics (CL) using linear regression. The slope (A), the intercept (B), the coefficient of determination (R^2), and the standard error of estimate (SEE) for the regression model $y = Ax + B$, where $y = \text{CL}$ and $x = \text{EC}$ are shown. The root-mean-squared error (RMS) between closure model predictions and measurements is also tabulated.

Closure	Regression	$\langle \bar{u} \rangle$	$\langle \overline{w'u'} \rangle$	$\langle \overline{u'u'} \rangle$	$\langle \overline{w'w'} \rangle$	q	$\langle \overline{w'u'u'} \rangle$	$\langle \overline{w'w'w'} \rangle$	$\langle \overline{w'u'w'} \rangle$
2nd	A	1.1	0.80	0.70	0.60	0.57	0.11	0.2	0.11
	B	-0.37	-0.09	0.36	0.43	0.71	-0.03	-0.07	0.03
	SEE	0.32	0.14	0.19	0.06	0.23	0.19	0.91	0.07
	R^2	0.98	0.92	0.92	0.95	0.91	0.10	0.37	0.31
	RMS	0.11	0.02	0.08	0.03	0.31	0.48	0.11	0.27
3rd	A	1.1	0.77	0.69	0.60	0.57	0.17	0.17	0.13
	B	-0.41	-0.11	0.39	0.42	0.72	-0.03	-0.08	0.032
	SEE	0.32	0.13	0.18	0.07	0.22	0.2	0.09	0.10
	R^2	0.98	0.93	0.92	0.96	0.92	0.19	0.29	0.24
	RMS	0.13	0.023	0.08	0.03	0.31	0.42	0.11	0.26

moments, particularly $\overline{\langle w'^3 \rangle}$. Recall that the vertical velocity variance budget, given by

$$-\frac{d}{dz}(\overline{\langle w'w'w' \rangle}) - \frac{q}{3\lambda_2} \left(\overline{\langle w'^2 \rangle} - \frac{q^2}{3} \right) - \frac{2}{3} \frac{q^3}{\lambda_3} = 0, \quad (7)$$

suggests that $\overline{\langle w'^2 \rangle}^{1/2}$ is affected directly by the gradient of $\overline{\langle w'^3 \rangle}$, especially for flow regions where q is small. For these two reasons, a comparison between the measured triple-velocity correlation tensor and predictions made using the third-moment budget is performed. The gradient-diffusion calculations (of the second-order model) are also shown for comparison and are presented in Table II.

In Figure 2a, the measured ensemble of $\overline{\langle w'u'u' \rangle}$, $\overline{\langle w'^3 \rangle}$, $\overline{\langle w'u'w' \rangle}$ are compared with predictions from gradient-diffusion theory and third-moment budgets (see Table II). For $\overline{\langle w'^3 \rangle}/u_*^3$, both closure model predictions agree with each other but significantly underestimate the vertical velocity skewness found in the measurements (by about 80%). The closure model agreement with each other is not surprising since the zero-fourth cumulant expansion does not introduce any ‘‘non-local’’ contribution to $\overline{\langle w'^3 \rangle}$, as evidenced by Equation (6). That is, the third-order closure model of Meyers and Paw U (1986) can be reduced to a gradient-diffusion model for $\overline{\langle w'^3 \rangle}$. The modelled $\overline{\langle w'^3 \rangle}$ profile by both closure models result in $d\overline{\langle w'^2 \rangle}/dz$ magnitudes smaller than the observed values, which is consistent with the overestimation of $\overline{\langle w'^2 \rangle}^{1/2}$ noted in Figure 2. Specifically, the modeled $d\overline{\langle w'^2 \rangle}/dz$ near $z/h = 0.4$ is underestimated by a factor of 5 (see Figure 2b). In these lower canopy layers, q is small (see Figure 1) and the flux transport term is the most important term for sustaining turbulence, and hence, the modeled profiles of $\overline{\langle w'^2 \rangle}^{1/2}$ are markedly influenced by $d\overline{\langle w'^3 \rangle}/dz$.

This point will be further discussed in Section 4.3, which considers the individual components of the turbulent kinetic energy budget.

For $\overline{\langle w'u'u' \rangle}$ and $\overline{\langle w'u'w' \rangle}$ profiles, the third-order closure shows minor improvements over second-order closure, though the disagreement with measurements remains large (up to 90% underestimation as evidenced by Table II). In fact, for the upper canopy component ($z/h > 0.6$), both closure models fail to reproduce the measured profiles to within a standard deviation. For comparison, Figure 2a includes the $\overline{\langle w'u'w' \rangle}/u_*^3$ from the maize canopy of Meyers and Paw U (1986) (see ‘+’ symbols), the corn canopy of Shaw and Seginer (1987) (see ‘*’ symbol), and the deciduous forest of Meyers and Baldocchi (1991) (see ‘x’ symbol). These measurements all suggest that $\overline{\langle w'u'w' \rangle}/u_*^3$ does not vanish close to $z/h = 1$ (in fact the data in Meyers and Baldocchi, 1991, peaks at $z/h = 1$). Both closure model predictions result in $\overline{\langle w'u'w' \rangle}/u_*^3 \rightarrow 0$ as $z/h \rightarrow 1.1$, which is

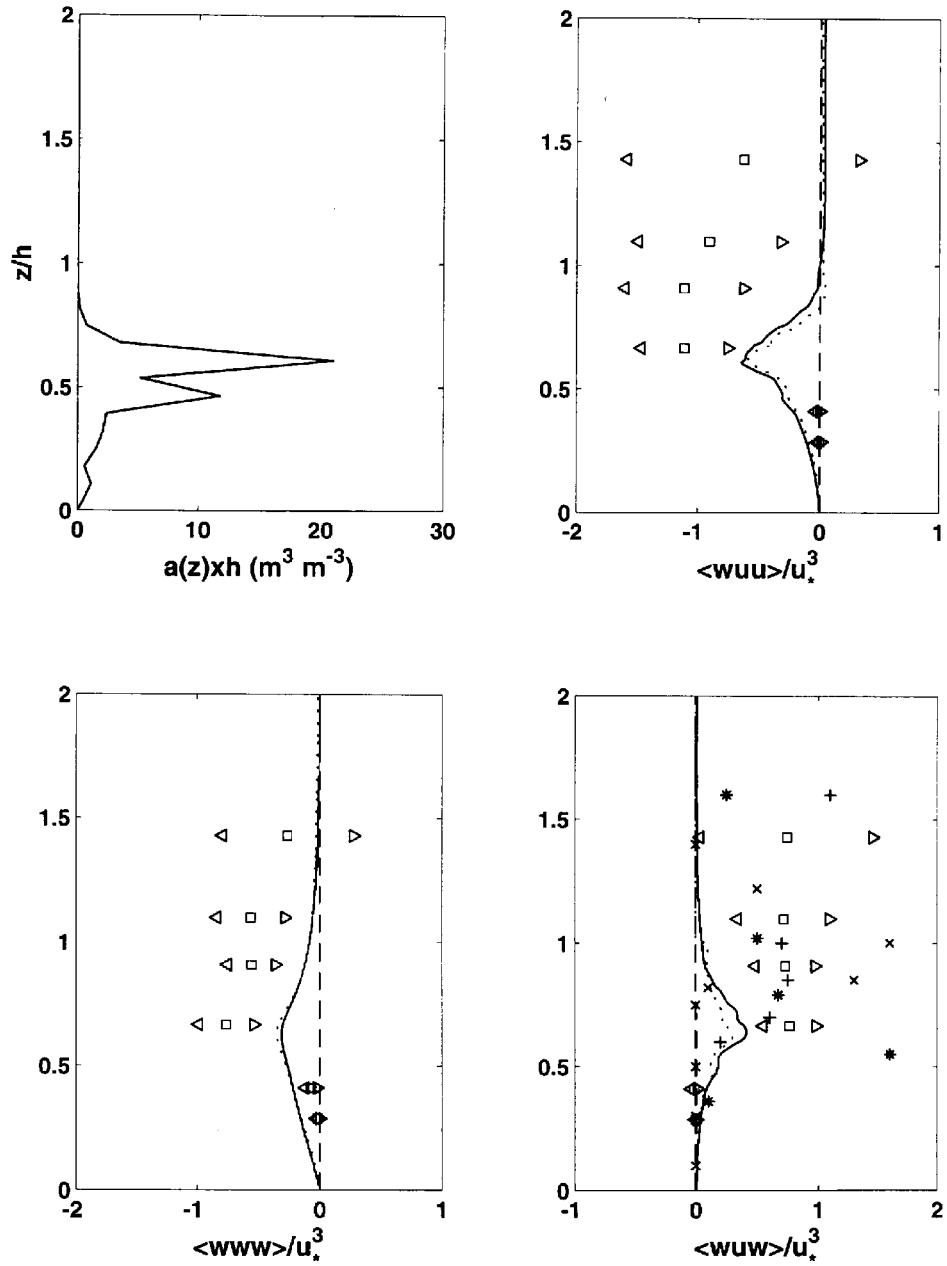


Figure 2a. Same as Figure 1 but for $\overline{w'u'w'}$, $\overline{w'u'u'}$, and $\overline{w'^3}$. The '+' symbols represent the maize measurements in Meyers and Paw U (1986), the '*' symbols represent the corn measurements of Shaw and Seginer (1987), and the 'x' symbols represent the measurements of Meyers and Baldocchi (1991).

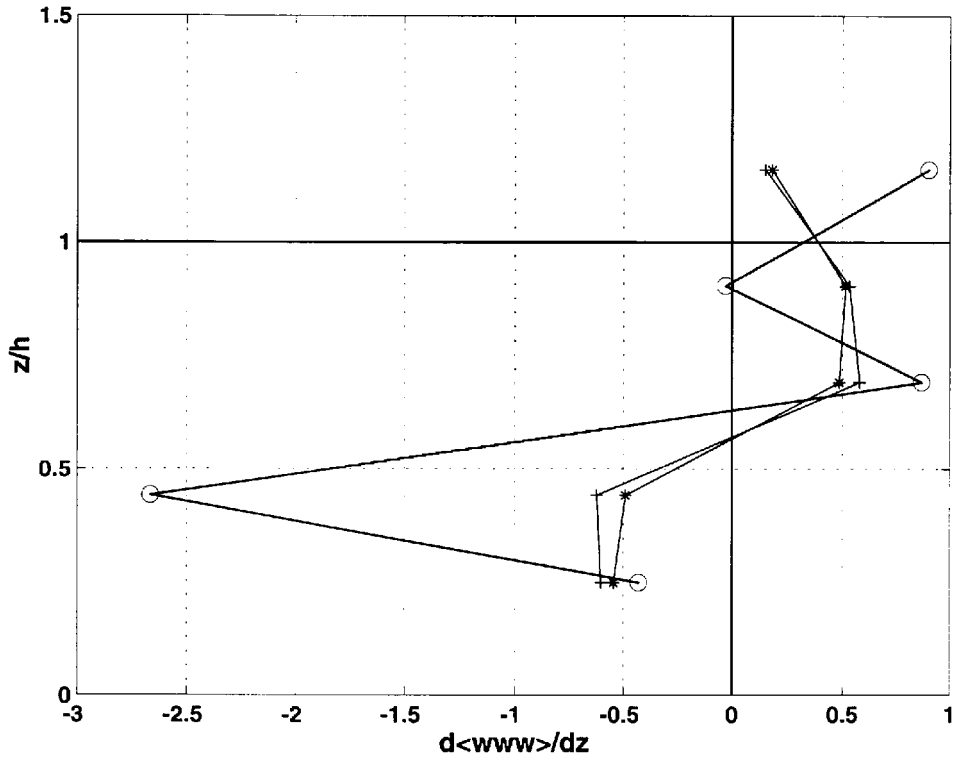


Figure 2b. Comparison between measured (open circles) and modeled $\overline{\langle w'^3 \rangle}$ gradients. The '+'s are $\overline{\langle w'^3 \rangle}$ gradients from the third-order closure model computed using the same heights as the measurements, while the '*' are from the second-order closure model.

unrealistic. In Raupach (1981), Shaw et al. (1983), and Katul et al. (1997b), it was demonstrated that the dimensionless moments (M_{3ij}), defined by

$$\frac{\overline{\langle w'u'_i u'_j \rangle}}{\sigma_w \sigma_{u_i} \sigma_{u_j}} = M_{3ij} = a_{ij} \Delta S_o;$$

where

$$\Delta S_o = \frac{\overline{\langle w'u' \rangle}^{(2)} - \overline{\langle w'u' \rangle}^{(4)}}{\overline{\langle w'u' \rangle}}$$

$$\overline{\langle w'u' \rangle}^{(k)} = \overline{\langle I_k u' w' \rangle}$$

$$I_2 = \begin{cases} 1 & \text{if } w' < 0, u' > 0 \quad (\text{sweep}) \\ 0 & \text{otherwise} \end{cases}$$

$$I_4 = \begin{cases} 1 & \text{if } w' > 0, u' < 0 \quad (\text{ejection}) \\ 0 & \text{otherwise} \end{cases}$$

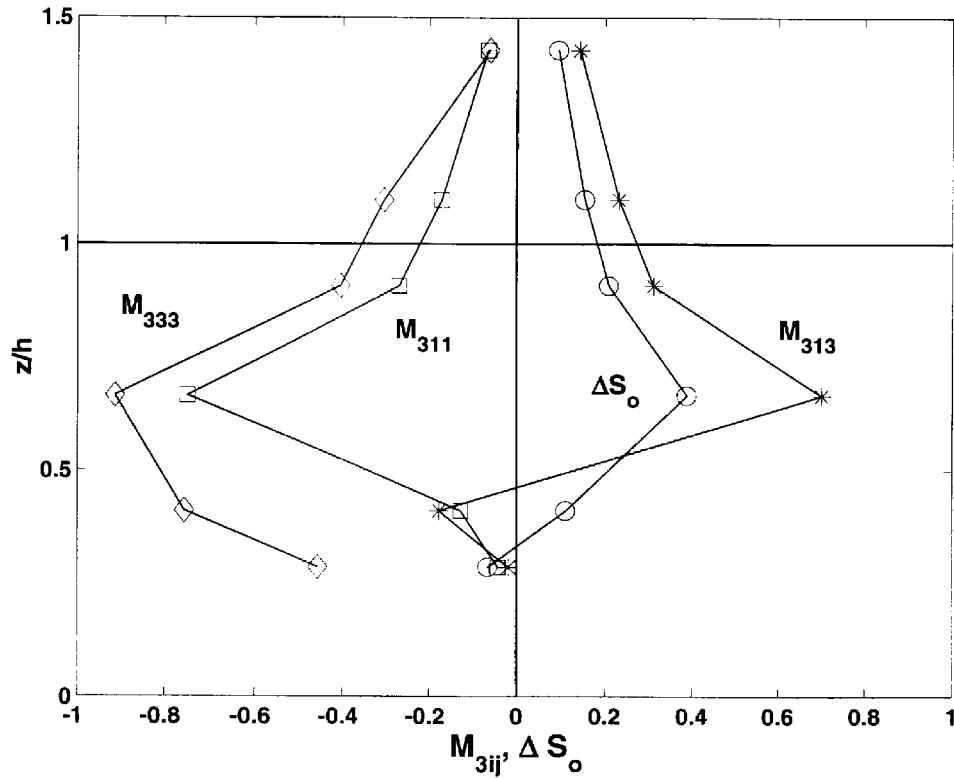


Figure 2c. The profiles of measured M_{3ij} and ΔS_o within and above the canopy. A positive ΔS_o at height z indicates that sweeps give the dominant contribution to $\overline{\langle u'w' \rangle}$ locally.

are functions of ΔS_o . Here, ΔS_o represents the relative contribution of the ejection and sweep eddy motions on the mean momentum flux. The magnitude of ΔS_o is strongly influenced by large excursions in w' , u' associated with gusts in the free air stream above the canopy. The double-overbar is a conditional average over non-zero values of I_k , I_k is the indicator function, and a_{ij} are constants derived from experiments. In Figure 2c, the measured ΔS_o ensemble profile along with the dimensionless moments M_{3ij} are shown. In agreement with numerous field experiments (see Katul et al., 1997b, for review), sweeps dominate the momentum transport mechanics in the canopy sublayer ($z/h = 0.3-1.5$). Such sweeping motion is dominated by intense, intermittent, downward-moving gusts emanating from above the canopy with a characteristic length scale comparable to h (Raupach, 1988). It is clear from Figure 2c that the ΔS_o profile describes well the third-order moment profiles (see Table III for details) suggesting that profiles of $\overline{\langle w'u'_i u'_j \rangle}$ are strongly influenced by such sweeping motion. Hence, this analysis demonstrates that closure models that can explicitly consider the ejection-sweep properties, with its 'course-grain' length scale may be better suited to model $\overline{\langle w'u'_i u'_j \rangle}$ than 'fine-grain' gradient-diffusion models.

TABLE III

Statistical analysis of the influence of sweeping motion, as modeled by ΔS_o , on M_{3ij} . The regression model $M_{3ij} = a_{ij} \Delta S_o + b_{ij}$ is used. The coefficient of determination (R^2) and the standard error of estimate (SEE) are also shown. Values in square brackets are calculated from Raupach's (1981) wind tunnel experiment.

M_{3ij}	Slope (a_{ij})	Intercept (b_{ij})	R^2	SEE
M_{311}	-1.62; [-2.7]	0.003	0.84	0.12
M_{322}	-1.18; [N/A]	-0.02	0.71	0.13
M_{333}	-1.04; [-1.6]	-0.32	0.25	0.29
M_{313}	+1.72; [1.4]	-0.06	0.72	0.18

Despite this failure of gradient-diffusion closure, the modelled $\overline{\langle u'w' \rangle}$, and $\overline{\langle u'^2 \rangle}^{1/2}$ profiles within the upper canopy layers agree with the measurements. As we demonstrate in Section 4.3, turbulence in these upper canopy layers is influenced by many other mechanisms (e.g., shear and wake-production), which tends to reduce the sensitivity of $\overline{\langle u'w' \rangle}$ and $\overline{\langle u'^2 \rangle}$ profiles to the modeling of $\overline{\langle w'u'u' \rangle}$ and $\overline{\langle w'u'w' \rangle}$. The failure of the third-order closure model to reproduce $\overline{\langle w'u'w' \rangle}$ in the upper canopy layers is at variance with earlier analysis by Meyers and Paw U (1986), who concluded that the third-order closure model reproduced well the measured $\overline{\langle w'u'w' \rangle}$ inside the canopy. We proceed to investigate whether the third-order closure model's failure in reproducing $\overline{\langle w'u'w' \rangle}/w_*^3$ is due to the truncation of cumulants at fourth order or due to the parameterizations involved in the other terms of the $\overline{\langle w'u'_i u'_j \rangle}$ budget.

4.2. THE ZERO-FOURTH CUMULANT APPROXIMATION

Whether the use of the zero-fourth cumulant approximation is valid for high Reynolds number flows is somewhat controversial. As discussed in Monin and Yaglom (1975, p. 407) and Brodkey (1967, pp. 300–301), the truncation of cumulants can lead to non-physical solutions which conflict with the requirement that the spectrum of moments be everywhere non-negative. However, such expansions have modelled well some higher-order moments (Antonia and Luxton, 1974), and were successful in linking the ejection-sweep properties to the triple-velocity correlations as was demonstrated by Nakagawa and Nezu (1977), Wyngaard and Sundararajan (1977), Raupach (1981), Shaw et al. (1983), Baldocchi (1989), Nagano and Tagawa (1990), and more recently in Katul et al. (1997b). These studies demonstrated that retaining the few important cumulants is sufficient to capture many basic flow properties. In Figure 3, measured and predicted profiles

of $\overline{\langle w^4 \rangle}$, $\overline{\langle u^4 \rangle}$, $\overline{\langle w^3 u' \rangle}$, $\overline{\langle w^2 u'^2 \rangle}$, $\overline{\langle w' u'^3 \rangle}$ are compared for all 69 runs. The normalization in Figure 3 was not based on u_* , but was applied such that the w' and u' time series have zero mean and unit variance. While the zero-fourth cumulant expansion reasonably reproduced measurements at 5 levels (in agreement with Meyers and Baldocchi, 1991), it failed to reproduce measurements at $z = 9.65$ m, which neighbors the level of maximum LAI. Recall from Figure 2a that this height is the most important level since the predicted peaks in $\overline{\langle w' u' w' \rangle}$, $\overline{\langle w' u' u' \rangle}$, and $\overline{\langle w'^3 \rangle}$ occur in its vicinity. What remains to be investigated is what processes are most significant in different regions of the canopy and whether these processes inject ‘added sensitivity’ to the parameterization of $\overline{\langle u'_i u'_j u'_k \rangle}$. For this purpose, components of the turbulent kinetic energy budget are considered.

4.3. COMPONENTS OF THE TURBULENT KINETIC ENERGY BUDGET

The modelled components of the turbulent kinetic energy budget profiles of shear production (P_{shear}), wake production (P_{wake}), dissipation ($P_{\text{dissipation}}$), and turbulent transport ($P_{\text{transport}}$) are shown in Figure 4 for both closure models. The normalization in Figure 4 is based on u_* and h for velocity and length scales, respectively.

As expected, the third-order closure model correctly predicted a negative P_{transp} while the second-order closure model predicted an unrealistic $P_{\text{transport}} = 0$ near $z = h$. Both closure models correctly simulated a positive $P_{\text{transport}}$ in the sub-canopy suggesting that inside the deeper canopy layers, turbulence is sustained by this term (see review by Kaimal and Finnigan, 1994; Meyers and Baldocchi, 1991). As evidenced from Figure 4, the wake and shear production terms are negligible in comparison to the dissipation and transport terms for $z/h < 0.4$ (i.e., below the bulk of the foliage), corresponding to low values of q in this region. It is for this reason that the modelled $\overline{\langle w'^2 \rangle}$ is so sensitive to the parameterization of the $\overline{\langle w'^3 \rangle}$ gradient noted in Figures 1 and 2a,b (for $z/h < 0.4$). In the upper canopy layers, shear and wake production (both of which are strictly functions of first and second moments) become the main contributors to the turbulent kinetic energy budget; hence, the sensitivity of $\overline{\langle u' w' \rangle}$, $\overline{\langle u'^2 \rangle}^{1/2}$ and $\overline{\langle w'^2 \rangle}^{1/2}$ to the parameterization of the triple-velocity correlation is reduced. Although the turbulent kinetic energy budget of Figure 4 is not explicitly used in Lagrangian stochastic models, such calculations do provide a framework for assessing which regions of the canopy flow domain are likely to be sensitive to errors in closure approximations for a given leaf area density profile.

5. Conclusions

This study demonstrated the following:

- (1) For modelling $\overline{\langle \bar{u} \rangle}$, $\overline{\langle u' w' \rangle}$, $\overline{\langle u'^2 \rangle}^{1/2}$, $\overline{\langle w'^2 \rangle}^{1/2}$ in plant canopies, no clear advantage is evident in closing the equations of motions beyond order 2.

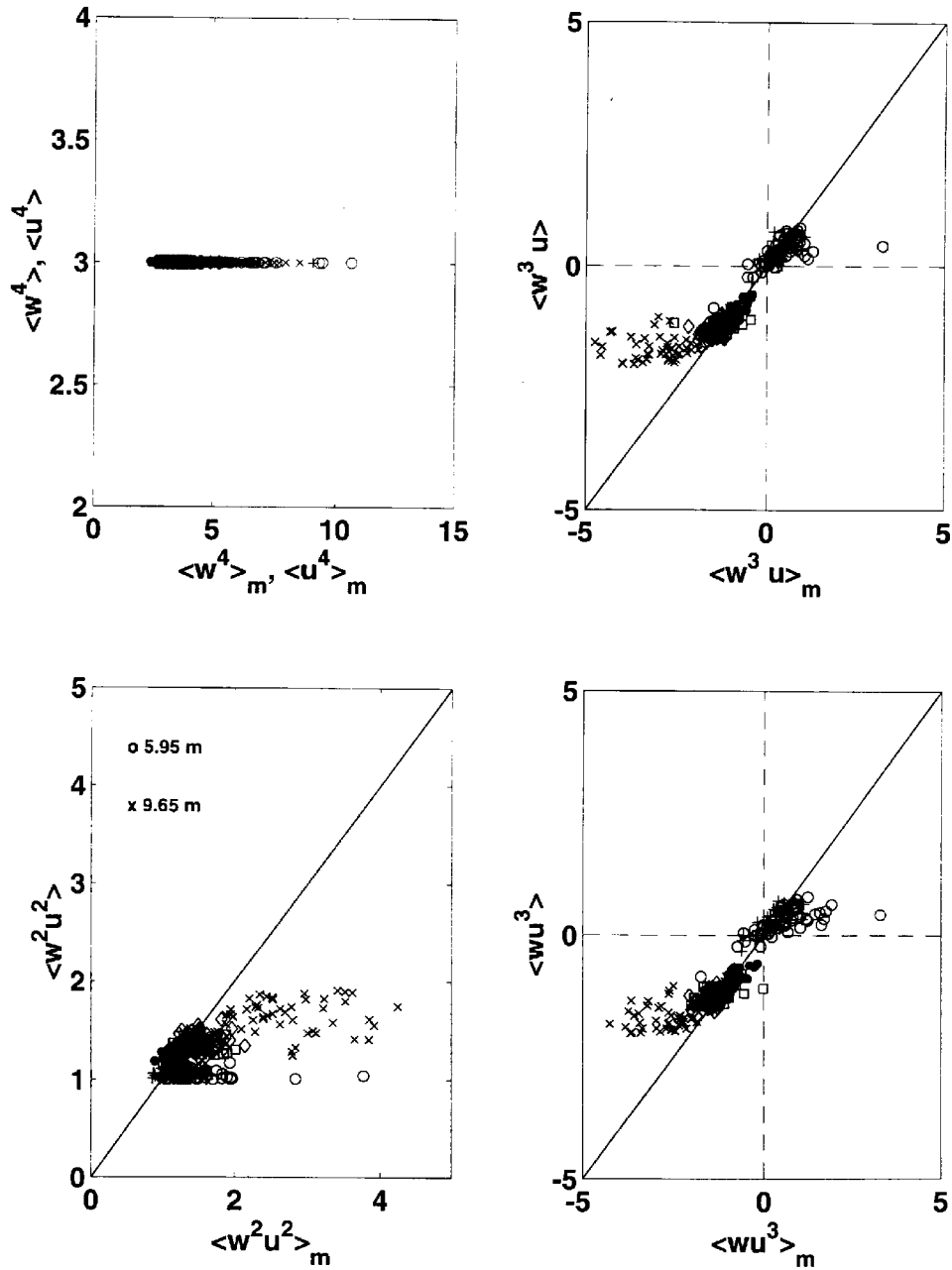


Figure 3. A comparison between measured (X_m denotes a measured X variable) and modelled fourth moments by the cumulant expansion method for all 69 runs and all six levels (plus is for 4.15 m; open circle is for 5.95 m; cross is for 9.65 m; open square is for 13.16 m; diamond is for 15.91 m; solid dot is for 20.7 m). The 1 : 1 line is also shown.

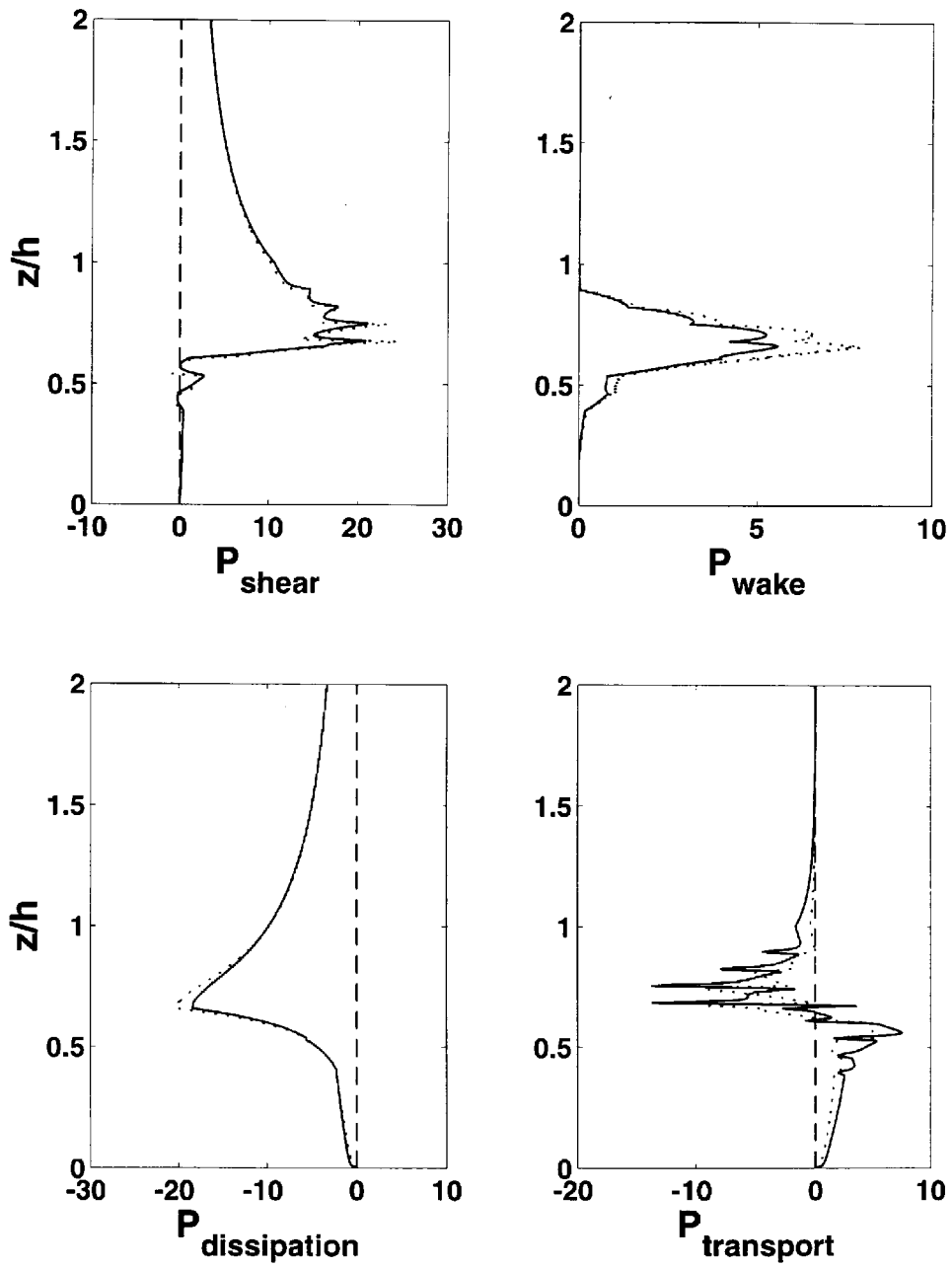


Figure 4. Components of the turbulent kinetic energy budget for the second- (dotted line) and third- (solid line) order closure models.

(2) Good agreement between measured and predicted profiles of $\langle \bar{u} \rangle$ and $\langle \overline{u'w'} \rangle$ by the two closure models was noted, in agreement with previous experiments over shorter vegetation.

(3) For the lower canopy layers ($z/h < 0.4$), the modelled $\langle \overline{w'^2} \rangle^{1/2}$ did not agree well with the measurements, although better agreement was noted for the upper canopy layers ($z/h > 0.6$). The systematic disagreement between closure model predictions and the measurements for the lower canopy layers is also evident for shorter vegetation and a deciduous forest. This disagreement is attributed, in part, to the sensitivity of these statistics to the flux transport parameterization in these layers.

(4) Both, second- and third-order closure models failed to reproduce the measured values of $\langle \overline{w'u'w'} \rangle$, $\langle \overline{w'u'u'} \rangle$, and $\langle \overline{w'^3} \rangle$ close to the canopy-atmosphere interface. This trend is consistent with the measurements and model results of Meyers and Baldocchi (1991) for a deciduous forest.

(5) The measured profiles of $\langle \overline{w'u'w'} \rangle / u_*^3$ from this experiment suggest that this statistic is significant in magnitude just above the canopy ($z/h = 1 - 1.2$) in agreement with other experiments. The second- and third-order closure models are unable to capture this. As demonstrated by Katul et al. (1997b), Shaw et al. (1983), Raupach (1981), and Nakagawa and Nezu (1977), this moment is controlled by the relative contributions of ejections to sweeps; hence, Reynolds-stress closure models that account for non-local effects (e.g., ejection-sweep cycle) are necessary to achieve proper closure for $\langle \overline{w'u'w'} \rangle$.

(6) The application of a zero-fourth cumulant approximation is reasonable near the canopy-atmosphere interface in agreement with earlier conclusions by Meyers and Baldocchi (1991) and Shaw and Seginer (1987) but it failed to reproduce the measured $\langle \overline{u'_i u'_j u'_k u'_l} \rangle$ by a factor of 2 to 3 at the maximum leaf area index level. This result is also in qualitative agreement with Shaw and Seginer (1987).

Acknowledgements

The authors would like to thank Cheng-I Hsieh for his assistance at the Duke Forest and in the data collection and analysis, David Ellsworth for providing the LAI profile, and Roger Shaw for the helpful discussion about the second-order closure model. A major portion of this work was done when the first author was on a junior sabbatical leave from the School of the Environment, Duke University. This project was funded, in part, by the U.S. Department of Energy (DOE) through their Southeast Regional Center at the University of Alabama, Tuscaloosa (DOE Cooperative Agreement DE-FCO3 90 ER6 10101) and through the FACE-FACTS project, and the National Science Foundation (NSF grant BIR-12333)

Appendix A. Determination of the Closure Constants and Computational Algorithm

A.1. DETERMINATION OF a_2 , a_3 , AND C

In the neutral atmospheric surface layer (ASL), the basic equations in the Wilson and Shaw (1977) model can be matched asymptotically to reproduce the flow statistics since: (1) gradients in triple-velocity correlations are negligible, (2) the velocity standard deviations $\sigma_{u_i} = \sqrt{u_i'^2}$ vary linearly with u_* , (3) the mean velocity gradient varies with u_* and z , and (4) the characteristic length $L(z) = kz$. Starting with

$$\sigma_u = A_u u_*$$

$$\sigma_v = A_v u_*$$

$$\sigma_w = A_w u_*$$

$$q = \sqrt{(A_u^2 + A_v^2 + A_w^2)u_*} = A_q u_*$$

$$\frac{du}{dz} = \frac{u_*}{kz}; \quad u_*^2 = -\overline{u'w'}$$

where A_u , A_v , and A_w are known (e.g., Shaw et al., 1974), a relationship between a_2 , a_3 , and C as a function of A_u , A_v , and A_w can be derived. By replacing the above surface-layer approximations in the Wilson and Shaw (1977) closure model for $\overline{u'w'}$, $\overline{w'w'}$, and $\overline{u'u'}$ we obtain:

$$a_2^{-1} \left(A_w^2 - \frac{A_q^2}{3} \right) + a_3^{-1} (2A_q^2) + C(0) = 0$$

$$a_2^{-1} \left(A_u^2 - \frac{A_q^2}{3} \right) + a_3^{-1} (2A_q^2) + C(0) = \frac{6}{A_q}$$

$$a_2^{-1} \left(\frac{1}{3A_q} \right) + a_3^{-1} (0) + C(1) = \left(\frac{A_w}{A_q} \right)^2.$$

These three equations can be solved for a_2 , a_3 , and C . From the measurements in Shaw et al. (1974), $A_u = 1.87$, and $A_v = A_w = 1.22$ resulting in $a_2 = 0.85$, $a_3 = 16.58$, and $C = 0.0771$.

A.2. DETERMINATION OF a_i

Assuming that $q\lambda_1 = kz u_*$ and noting that $\lambda_1 = a_1(kz)$ in the ASL results in $a_1 = 1/A_q$. For the measurements by Shaw et al. (1974), $A_q = (6.5)^{1/2}$ and $a_1 = 0.392$. As evident, the constants a_1 , a_2 , a_3 , and C are dependent on A_u , A_v , and A_w . We decided not to use directly our measured A_u , A_v , and A_w to further examine the applicability of a_1 , a_2 , a_3 , and C for stands very different from the maize canopy of Shaw et al. (1974). Furthermore, by computing these constants using another data set, all the 6 levels can be used in the comparison between model predictions and measurements vis-à-vis the anchoring of variances at the highest measurement level of the present experiment.

A.3. DETERMINATION OF α AND C_d

Since α and C_d are dependent on the canopy rather than flow properties, we chose the optimum combination of α and C_d such that the simulated and measured $\langle \bar{u} \rangle$ have the least standard error of estimate. In these models, C_d and α were permitted to vary from 0.10 to 0.35 and 0.05 to 0.2, respectively. The resulting optimum parameter combinations are $C_d = 0.20$ and $\alpha = 0.14$. The optimized C_d (constant with depth) is in good agreement with other C_d values reported for a Ponderosa pine forests (= 0.16 in Li et al., 1986). An estimate of C_d by Massman (1987) for a mature Scots pine of Halldin and Lindroth (1986) resulted in a high C_d (= 0.3) value. The $C_d = 0.3$ estimate did not consider shelter effects correction (Raupach and Thom, 1981) which tend to appreciably reduce C_d . However, $\alpha = 0.14$ was larger than the Wilson and Shaw (1977) value for maize by a factor of 2.

A.4. NUMERICAL TECHNIQUES

The computational flow domain was set to 2 h, with $\Delta z = 0.05$ cm resulting in 560 grid nodes, where Δz is the grid node spacing. This grid density was necessary due to the variability in LAI profile. Also, with such a small Δz , smoothness and capturing all variability in the gradients is likely. Boundary conditions were specified as:

$$z = 0 \left\{ \begin{array}{l} \sigma_u = 0 \\ \sigma_v = 0 \\ \sigma_w = 0 \\ u_* = 0 \\ \langle \bar{u} \rangle = 0 \end{array} \right.$$

$$z = 2h \left\{ \begin{array}{l} \sigma_u = A_u u_* \\ \sigma_v = A_v u_* \\ \sigma_w = A_w u_* \\ u_* = 1 \\ \langle \bar{u} \rangle = A_m u_*, \end{array} \right.$$

where A_u , A_v , and A_w are from Shaw et al. (1974), and A_m at $z/h = 2.0$ is determined by extrapolating logarithmically the value measured at $z/h = 1.47$ by the Gill sonic anemometer. The five ordinary differential equations (ODEs) in Equation (4) were first discretized by central differencing of all derivatives. An implicit numerical scheme was constructed for each ODE with the boundary conditions stated above. The tridiagonal system, resulting from the implicit forms of these discretized equations, was solved using the *Tridag* routine in Press et al. (1992, pp. 42–43) for each second order ODE to produce the turbulent statistic profile. Profiles for all variables were initially assumed and a variant of the relaxation scheme described in Wilson (1988) was used for all computed variables. Relaxation factors as small as 5% were necessary in the iterative scheme because of the irregularity in the LAI profile. Convergence is achieved when the maximum difference between two successive iterations for q did not exceed 0.1%. The same procedure was adopted for the third-order closure model. We ran the closure models for $\Delta z = 0.01, 0.02, 0.05,$ and 0.1 cm and checked that all solutions were independent of Δz .

Appendix B. Reduction of Fourth Moments to Second Moments via Zero-Fourth Cumulant Expansions

The relationship between central moments and cumulants of order 4 is given by (Monin and Yaglom, 1971, p. 230; Gardiner, 1983, p. 35):

$$\langle\langle X_1 X_2 X_3 X_4 \rangle\rangle = C_0 - C_1 + 2C_2 - 6C_3,$$

where $\langle\langle \cdot \rangle\rangle$ indicates a cumulant operator, $\langle \cdot \rangle$ indicates an averaging operator, $X_1, X_2, X_3,$ and X_4 are arbitrary variables, and $C_0, C_1, C_2,$ and C_3 are given by:

$$C_0 = \langle X_1 X_2 X_3 X_4 \rangle$$

$$C_1 = D_1 + D_2$$

$$D_1 = \langle X_1 \rangle \langle X_2 X_3 X_4 \rangle + \langle X_2 \rangle \langle X_1 X_3 X_4 \rangle + \langle X_3 \rangle \langle X_1 X_2 X_4 \rangle \\ + \langle X_4 \rangle \langle X_1 X_2 X_3 \rangle$$

$$D_2 = \langle X_1 X_2 \rangle \langle X_3 X_4 \rangle + \langle X_1 X_3 \rangle \langle X_2 X_4 \rangle + \langle X_2 X_3 \rangle \langle X_1 X_4 \rangle$$

$$C_2 = \langle X_1 \rangle \langle X_2 \rangle \langle X_3 X_4 \rangle + \langle X_1 \rangle \langle X_3 \rangle \langle X_2 X_4 \rangle + \langle X_1 \rangle \langle X_4 \rangle \langle X_2 X_3 \rangle \\ + \langle X_2 \rangle \langle X_3 \rangle \langle X_1 X_4 \rangle + \langle X_2 \rangle \langle X_4 \rangle \langle X_1 X_3 \rangle + \langle X_3 \rangle \langle X_4 \rangle \langle X_1 X_2 \rangle$$

$$C_3 = \langle X_1 \rangle \langle X_2 \rangle \langle X_3 \rangle \langle X_4 \rangle.$$

Upon substituting u' and w' for their corresponding X_1 , X_2 , X_3 , and X_4 , assuming that the fourth cumulant $\langle\langle X_1 X_2 X_3 X_4 \rangle\rangle$ is zero, noting that $\overline{\langle u' \rangle} = \overline{\langle w' \rangle} = 0$, and after some algebra, the following relations are derived:

$$\overline{\langle w'^4 \rangle} = 3\overline{\langle w'^2 \rangle}^2$$

$$\overline{\langle w'^3 u' \rangle} = 3\overline{\langle w'^2 \rangle} \overline{\langle u' w' \rangle}$$

$$\overline{\langle w'^2 u'^2 \rangle} = \overline{\langle w'^2 \rangle} \overline{\langle u'^2 \rangle} + 2\overline{\langle u' w' \rangle}^2$$

$$\overline{\langle w' u'^3 \rangle} = 3\overline{\langle u'^2 \rangle} \overline{\langle u' w' \rangle}$$

$$\overline{\langle u'^4 \rangle} = 3\overline{\langle u'^2 \rangle}^2.$$

These relations are tested in Figure 3 for all six levels.

References

- André, J. C., Lacarrere, P., and Traore, K.: 1981, 'Pressure Effects on Triple Correlations in Turbulent Convective Flows', in *Turbulent Shear Flows III*, Springer-Verlag, Berlin, pp. 243–252.
- Albini, F. A.: 1981, 'A Phenomenological Model for Wind Speed and Shear Stress Profiles in Vegetation Cover Layers', *J. Appl. Meteorol.* **20**, 1325–1335.
- Antonia, R. A. and Luxton, R.E.: 1974, 'Characteristics of Turbulence within an Internal Boundary Layer', *Adv. Geophys.* **18A**, 263–285.
- Baldocchi, D.: 1989, 'Turbulent Transfer in a Deciduous Forest', *Tree Phys.* **5**, 357–377.
- Baldocchi, D.: 1992, 'A Lagrangian Random Walk Model for Simulation Water Vapor, CO₂ and Sensible Heat Densities and Scalar Profiles over and within a Soybean Canopy', *Boundary-Layer Meteorol.* **61**, 113–144.
- Brodkey, R. S.: 1967, *The Phenomena of Fluid Motions*, Dover Publications, 737 pp.
- Cionco, R. M.: 1965, 'A Mathematical Model for Air Flow in Vegetative Canopy', *J Appl. Meteorol.* **4**, 517–522.
- Cionco, R. M.: 1972, 'A Wind Profile Index for Canopy Flow', *Boundary-Layer Meteorol.* **3**, 255–263.
- Cowan, I. R.: 1968, 'Mass, Heat, and Momentum Exchange between Stands of Plants and their Atmospheric Environment', *Quart J. Roy. Meteorol. Soc.* **94**, 318–332.
- Deardorff, J. W.: 1978, 'Closure of Second and Third Moment Rate Equations for Diffusion in Homogeneous Turbulence', *Phys. Fluids* **21**, 525–530.
- Donaldson, C. Du P.: 1973, 'Construction of a Dynamic Model for the Production of Atmospheric Turbulence and the Dispersion of Atmospheric Pollutants', in *Workshop on Micrometeorology*, Amer. Meteorol. Soc., pp. 313–392.
- Ellsworth, D., Oren, R., Huang, C., Phillips, N., and Hendrey, G. R.: 1995, 'Leaf and Canopy Responses to Elevated CO₂ in a Pine Forest under Free Air CO₂ Enrichment', *Oecologia* **104**, 139–146.
- Gardiner, C. W.: 1983, *Handbook of Stochastic Methods for Physics, Chemistry, and the Natural Sciences*, Springer-Verlag, 442 pp.
- Hanjalic, K. and Launder, B. E.: 1972, 'A Reynold Stress Model for Turbulence and its Application to Thin Shear Flows', *J. Fluid Mech.* **52**, 609–638.

- Halidin, S. and Lindroth, A.: 1986, 'Pine Forest Microclimate Simulation Using Different Diffusivities', *Boundary-Layer Meteorol.* **35**, 103–123.
- Kaimal, J. C. and Finnigan, J.J.: 1994, *Atmospheric Boundary Layer Flows: Their Structure and Measurement*, Oxford Press, 289 pp.
- Katul, G. G., Oren, R., Ellsworth, D., Hsieh, C. I., Phillips, N., and Lewin, K.: 1997a, 'A Lagrangian Dispersion Model for Predicting CO₂ Sources, Sinks, and Fluxes in a Uniform Loblolly Pine (*Pinus taeda* L.) Stand', *J. Geophys. Res.* **102**, 9309–9321.
- Katul, G. G., Hsieh, C. I., Kuhn, G., Ellsworth, D., and Nie, D.: 1997b, 'Turbulent Eddy Motion at the Forest-Atmosphere Interface', *J. Geophys. Res.* **102**, 13,409–13,421.
- Kondo, J. and Akashi, S.: 1976, Numerical Studies on the Two-Dimensional Flow in Horizontally Homogeneous Canopy Layers', *Boundary-Layer Meteorol.* **10**, 255–272.
- Launder, B. E.: 1996, 'An Introduction to Single-Point Closure Methodology', in T. B. Gatski, M. Y. Hussaini, and J. L. Lumley (eds.), *Simulation and Modeling of Turbulent Flows*, ICASE/LaRC Series in Computational Science and Engineering, Oxford University Press, 314 pp.
- Launder, B. E., Reece, G. J., and Rodi, W.: 1975, 'Progress in the Development of a Reynolds-Stress Turbulence Closure', *J. Fluid Mech.* **68**, 537–566.
- Leclerc, M. Y., Thurtell, G. W., and Kidd, G. E.: 1988, Measurements and Langevin Tracer Concentration Fields Downwind from a Circular Source Inside an Alfalfa Canopy', *Boundary-Layer Meteorol.* **43**, 287–308.
- Lewellen, W. S., Teske, M. E., and Sheng, Y. P.: 1980, 'Micrometeorological Applications of a Second Order Closure Model of Turbulent Transport', in L. J. S. Bradbury, F. Durst, B. E. Launder, F. W. Schmidt, and J. H. Whitelaw (eds.), *Turbulent Shear Flows II*, Springer-Verlag, pp. 366–378.
- Li, Z. J., Miller, D. R., and Lin, J. D.: 1985, 'A First-Order Closure Scheme to Describe Counter-Gradient Momentum Transport in Plant Canopies', *Boundary-Layer Meteorol.* **33**, 77–83.
- Lumley, J. L.: 1978, 'Computational Modelling of Turbulent Flows', *Adv. Appl. Mech.* **18**, 123.
- Maitani, T.: 1978, 'On the Downward Transport of Turbulent Kinetic Energy in the Surface Layer over Plant Canopies', *Boundary-Layer Meteorol.* **14**, 571–584.
- Massman, W.: 1987, 'A Comparative Study of Some Mathematical Models of the Mean Wind Structure and Aerodynamic Drag of Plant Canopies', *Boundary-Layer Meteorol.* **40**, 179–197.
- Massman, W.: 1997, 'An Analytical One-Dimensional Model of Momentum Transfer by Vegetation of Arbitrary Structure', *Boundary-Layer Meteorol.* **83**, 407–421.
- Mellor, G.: 1973, 'Analytic Prediction of the Properties of Stratified Planetary Boundary Layer', *J. Atmos. Sci.* **30**, 1061–1069.
- Meyers, T. and Paw U, K. T.: 1986, 'Testing of a Higher-Order Closure Model for Modeling Airflow within and above Plant Canopies', *Boundary-Layer Meteorol.* **37**, 297–311.
- Meyers, T. and Baldocchi, D. D.: 1991, 'The Budgets of Turbulent Kinetic Energy and Reynolds Stress within and above Deciduous Forest', *Agric. For. Meteorol.* **53**, 207–222.
- Monin, A. S. and Yaglom, A. M.: 1971, *Statistical Fluid Mechanics*, MIT Press, Cambridge, MA, 769 pp.
- Monin, A. S. and Yaglom, A. M.: 1975, *Statistical Fluid Mechanics*, MIT Press, Cambridge, MA, 874 pp.
- Mulhearn, P. J. and Finnigan, J. J.: 1978, 'Turbulent Flow over a Very Rough Random Surface', *Boundary-Layer Meteorol.* **15**, 109–132.
- Nagano, Y. and Tagawa, M.: 1990, 'A Structural Turbulence Model for Triple Products of Velocity and Scalar', *J. Fluid Mech.* **196**, 157–185.
- Nagano, Y. and Tagawa, M.: 1996, 'Coherent Motion and Their Role in Transport Processes in a Wall Turbulent Shear Flow', in C. J. Chen, C. Shih, J. Lienau, and J. Kung (eds.), *Flow and Modeling of Turbulent Measurements VI*, Balkema, Rotterdam, pp. 17–28.
- Nakagawa, H. and Nezu, I.: 1977, 'Prediction of the Contributions to the Reynolds Stress from Bursting Events in Open Channel Flows', *J. Fluid Mech.* **80**, 99–128.

- Press, W. H., Teukolsky, S. A., Vetterling, W. T., and Flannery, B. P.: 1992, *Numerical Recipes in Fortran*, 2nd edn, Cambridge University Press, 963 pp.
- Raupach, M. R.: 1994, 'Simplified Expressions for Vegetation Roughness Length and Zero-Plane Displacement as Functions of Canopy Height and Area Index', *Boundary-Layer Meteorol.* **71**, 211–216.
- Raupach, M. R.: 1981, 'Conditional Statistics of Reynolds Stress in Rough-Wall and Smooth-Wall Turbulent Boundary Layers', *J. Fluid Mech.* **108**, 363–382.
- Raupach, M. R. and Thom, A. S.: 1981, 'Turbulence in and above Plant Canopies', *Ann. Rev. Fluid Mech.* **13**, 97–129.
- Raupach, M. R. and Shaw, R. H.: 1982, 'Averaging Procedures for Flow within Vegetation Canopies', *Boundary-Layer Meteorol.* **22**, 79–90.
- Raupach, M. R., Antonia, R. A., and Rajagopalan, S.: 1991, 'Rough-Wall Turbulent Boundary Layers', *Appl. Mech. Rev.* **44**, 1–25.
- Raupach, M. R., Denmead, O. T., and Dunin, F. X.: 1992, 'Challenges in Linking Atmospheric CO₂ Concentrations to Fluxes at Local and Regional Scales', *Aust. J. Bot.* **40**, 697–716.
- Raupach, M. R.: 1988, 'Canopy Transport Processes', in W. L. Steffen and O. T. Denmead (eds.), *Flow and Transport in the Natural Environment*, Springer-Verlag, New York, pp. 95–127.
- Sawford, B. L.: 1986, 'Generalized Random Forcing in Random-Walk Turbulent Dispersion Models', *Phys. Fluids* **29**, 3582–3583.
- Sawford, B. L. and Guest, F. M.: 1987, 'Lagrangian Stochastic Analysis of Flux-Gradient Relationship in the Convective Boundary Layer', *J. Atmos. Sci.* **44**, 1152–1165.
- Sellers, P. J., Mintz, Y., Sud, Y., and Dalcher, A.: 1985, 'A Simple Biosphere Model (SiB) for Use within General Circulation Models', *J. Atmos. Sci.*, **43**, 505–531.
- Shaw, R. H., 1977, 'Secondary Wind Speed Maxima Inside Plant Canopies', *J. Appl. Meteorol.* **16**, 514–521.
- Shaw, R. H., den Hartog, G., King, K. M., and Thurtell, G. W.: 1974, 'Measurements of Mean Wind Flow and Three-Dimensional Turbulence Intensity within a Mature Corn Canopy', *Agric. For. Meteorol.* **13**, 419–425.
- Shaw, R. H., Tavangar, J., and Ward, D.: 1983, 'Structure of the Reynolds Stress in a Canopy Layer', *J. Clim. Appl. Meteor.* **22**, 1922–1931.
- Shaw, R. H. and Seginer, I.: 1987, 'Calculation of Velocity Skewness in Real and Artificial Canopies', *Boundary-Layer Meteorol.* **39**, 315–332.
- Schumann, U.: 1977, 'Realizability of Reynolds Stress Turbulence Models', *Phys. Fluids* **20**, 721–726.
- Sreenivasan, K. R., Tavoularis, S., and Corrsin, S.: 1982, 'A Test of Gradient Transport and its Generalization', in L. J. S. Bradbury, F. Durst, B. E. Launder, F. W. Schmidt, and J. H. Whitelaw (eds.), *Turbulent Shear Flow III*, Springer-Verlag, New York, pp. 96–112.
- Taconet, O., Bernard, R., and Vidal-Madjas, D.: 1986, 'Evapotranspiration over an Agricultural Region Using a Surface Flux/Temperature Model Based on NOAA-AVHRR Data', *J. Clim. Appl. Meteorol.* **25**, 284–307.
- Thom, A. S.: 1971, 'Momentum Absorption by Vegetation', *Quart. J. Roy. Meteorol. Soc.* **97**, 414–428.
- Wilson, J. D.: 1988, 'A Second Order Closure Model for Flow through Vegetation', *Boundary-Layer Meteorol.* **42**, 371–392.
- Wilson, J. D.: 1989, 'Turbulent Transport within the Plant Canopy', in *Estimation of Areal Evapotranspiration*, IAHS Publ., No. 177, pp. 43–80.
- Wilson, N. R. and Shaw, R. H.: 1977, 'A Higher Order Closure Model for Canopy Flow', *J. Appl. Meteorol.* **16**, 1198–1205.
- Wyngaard, J. C. and Sundararajan, A.: 1977, 'The Temperature Skewness Budget in the Lower Atmosphere and its Implications to Modeling', in F. Durst, B. E. Launder, F. W. Schmidt, and J. H. Whitelaw (eds.), Springer-Verlag, New York, pp. 319–326.

Zeman, O. and Tennekes, H.: 1975, 'A Self Contained Model for the Pressure Terms in the Turbulent Stress Equation of the Neutral Atmospheric Boundary Layer', *J. Atmos. Sci.* **32**, 1808–1813.

Zeman, O. and Lumley, J. L.: 1976, 'Modeling Buoyancy Driven Mixed Layers', *J. Atmos. Sci.* **33**, 1974–1988.